Sustainable Carbon Materials

https://doi.org/10.48130/scm-0026-0017

Review

Open Access

A critical review of biomass-derived carbon anodes for potassium-ion batteries

Yongfeng Zhu, Xiaowen Liu, Jinze Dai and Qingang Xiong*

Received: 5 January 2026

Revised: 9 February 2026

Accepted: 27 March 2026

Published online: 23 April 2026

Abstract

The intensive consumption of lithium resources in recent years has spurred the development of alternative energy storage batteries to supplement or replace lithium-ion batteries. As one of the most promising candidates for large-scale energy storage in the foreseeable future, potassium-ion batteries feature lower costs and more plentiful potassium resources. However, the bulkier size of potassium ions induces sluggish reaction kinetics and inferior cycling stability in current commercial anodes. Advanced biomass-derived carbon anodes deliver superior potassium ion storage performance, benefiting from their intrinsically large specific surface areas, well-defined pore architectures, and abundant defect structures. While numerous studies have documented these anodes, a comprehensive review focusing on the fabrication of biomass-derived carbon anode materials for potassium-ion batteries remains notably lacking. In this review, we discuss a series of different biomass-derived carbon anodes, including their preparation methods, advantages, and disadvantages, and we propose prospects for future research. In addition, carbonization methods and activation techniques are discussed, together with their respective merits and limitations. This review aims to provide a comprehensive understanding of biomass-derived carbon anode materials for potassium-ion batteries and to guide the development of high-performance anode materials.

Keywords: Biomass, Carbon, Anodes, Potassium-ion batteries

Highlights

- Highlights the supplementary and alternative potential of PIBs compared to LIBs.
- Summarizes the working mechanisms and various anode materials used in PIBs.
- Elaborates on the merits and demerits of various BDCM anodes.
- Reviews the carbonization and activation methods for BDCMs.

Graphical abstract

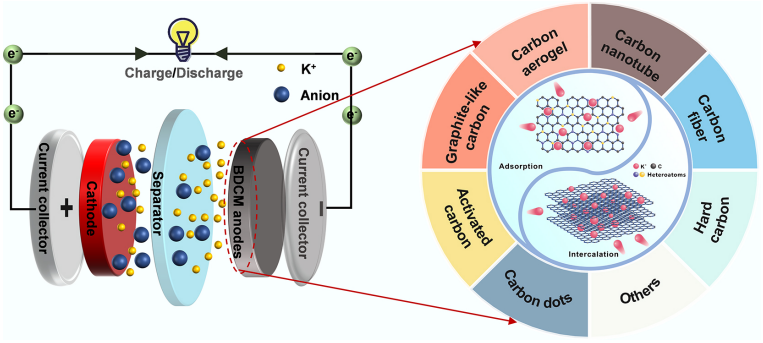

* Correspondence: Qingang Xiong (qingangxiong@scut.edu.cn)

Full list of author information is available at the end of the article.

https://doi.org/10.48130/scm-0026-0017

Introduction

With long cycle life, excellent high-rate capability, and high safety, lithium-ion batteries (LIBs) are currently the dominant energy storage solution and have been widely deployed in portable electronic devices, electric vehicles, and large-scale energy storage systems[1]. This has triggered massive consumption of lithium resources. However, because the reserves of lithium resources are rather limited (at the level of about 20 ppm within the earth's crust) and cannot meet the great demand in recent years, the price of lithium is getting more and more unaffordable[2,3]. Thus, it is urgently required to develop alternatives that have huge reserves but comparable performance to LIBs to complement and even replace LIBs.

Elements in the same group as lithium, sodium, and potassium are viewed as potential substitutes to build up ion batteries with comparable performance to LIBs[4]. As Table 1 shows, the reserves of sodium and potassium are far more abundant (about three orders of magnitude) than lithium, which inevitably results in a much lower price and is critical to long-term large-scale production of batteries. To date, many efforts have been devoted to developing suitable anode materials for PIBs. Besides, Na^+ and K^+ both exhibit lower desolvation energy between ions and solvent molecules in carbonate electrolytes than Li^+, which is highly beneficial to faster ionic transport of Na^+ and K^+ in electrolytes than Li^+ [5]. Table 1 also shows that the solvated ionic radius of Na^+ and K^+ is smaller than that of Li^+, which means higher ionic conductivity and diffusion coefficient in electrolytes[6]. It is widely accepted that faster ionic transport and lower desolvation energy lead to higher rate performance[7]. Thanks to these advantages, sodium-ion batteries (SIBs) and potassium-ion batteries (PIBs) hold great potential to complement the large-scale applications of LIBs.

Table 1 also shows that the voltage vs SHE, K/K^+ (−2.92 V) is lower than Na/Na^+ (−2.71 V), enabling PIBs to have a higher operating voltage and a higher energy density. Furthermore, the higher ionic conductivity of K^+ salt electrolytes and lower density of K metal lead to better rate performance and energy density of PIBs than SIBs. Therefore, the aforementioned compelling physicochemical properties of potassium make PIBs more feasible to be employed to substitute LIBs. To this end, PIBs have received much attention from both academic and industrial communities[15]. However, it can be clearly seen that the ionic radius of Li^+, Na^+, and K^+ is 0.68, 0.97, and 1.38 Å, respectively, so the anodes of PIBs usually undergo a larger volume change during the charge/discharge process than LIBs and SIBs, and damaged anodes would severely decrease the lifetime of PIBs[16,17].

Table 1 Physicochemical properties and abundance of lithium, sodium, and potassium

Physical/chemical properties	Lithium (Li)	Sodium (Na)	Potassium (K)
Abundance in earth crust (wt.%)[8]	0.0017	2.3	1.5
Cost of carbonate (US$ t^{-1})[9]	6,500	200	1,000
Cost of metals (US$ t^{-1})[9]	100,000	3,000	13,000
Desolvation energy in ethylene carbonate (KJ mol^{-1})[10]	208.9	152.8	114.6
Stokes radii in propylene carbonate (Å)[11]	4.8	4.6	3.6
Stokes radii in water (Å)[11]	2.38	1.84	1.25
Voltage vs SHE (V)[12]	−3.04	−2.71	−2.92
Conductivity of 1M Li/Na/KFSI in ethylene carbonate/diethyl carbonate (mS cm^{-1})[11]	9.3	9.7	10.7
Density (g cm^{-3})[13]	0.535	0.968	0.856
Ionic radius (Å)[14]	0.68	0.97	1.38

Thus, the development of suitable anode materials to decrease volume expansion and structural damage is one of the most critical tasks for PIBs[18]. To date, many efforts have been devoted to developing suitable anode materials for PIBs, and some research progress has been achieved[19].

Since K^+ can intercalate into the graphitic structure to form a KC_8 intercalation compound with a high theoretical capacity of 279 mAh g^{-1}, carbon materials (CMs) are widely investigated as anodes for PIBs[20]. CMs are traditionally and majorly prepared from non-renewable fossil fuels such as coal, coal pitch, and petroleum pitch. As the cost is relatively high and the environmental impact is obvious, using non-renewable fossil fuels to produce CMs for anode materials becomes more and more non-competitive[21]. As an abundant, carbon-neutral, and low-cost resource, non-food biomass has been widely viewed as the dominant replacement of non-renewable fossil fuels to synthesize CMs in the future[22,23]. Besides, biomass-derived CMs (BDCMs) inherently possess a large specific surface area, well-ordered pore structure, and abundant defect structures[24]. The large specific surface area and porous structure of CMs can provide tremendous active sites and a large contact area between anodes and electrolyte, shortening the ion transport path to achieve a high transmission rate[25]. The defects can supply extra adsorption sites for K^+ storage, showing a higher capacity than 279 mAh g^{-1}. Therefore, BDCMs have attracted widespread attention to develop high K^+ storage performance anodes for PIBs.

Recent studies have increasingly focused on BDCMs, and they have emerged as one of the most promising candidate anodes for PIBs. Given this, it is crucial to review the progress in utilizing BDCMs for PIB anodes and to identify future research directions. However, comprehensive reviews addressing the production of anode materials for PIBs using BDCMs are still scarce. In this review, the working principle of PIBs is first introduced, and common anode materials for PIBs are summarized. Then, different BDCMs used as anode materials for PIBs are comprehensively reviewed, with an analysis of the pros and cons of each type. Furthermore, the preparation methods and activation techniques are discussed, along with their respective advantages and limitations. Finally, critical issues that BDCMs face as anode materials for PIBs are highlighted, and perspectives on potential approaches and strategies to address these challenges are provided. This review not only surveys the current advancements in BDCMs but also suggests several research directions for developing high-performance anode materials for PIBs.

PIBs

Configuration and operational mechanism

Figure 1 illustrates the schematic configuration and operational mechanism of a typical PIB[26]. Like LIBs, PIBs consist of three essential components: the anode, cathode, and electrolyte. PIBs are rocking-chair batteries, where potassium ions serve as charge carriers, migrating between the anode and cathode during charging and discharging. During charging, potassium ions are deintercalated from the cathodes, migrate through the electrolyte, and then intercalate into the carbon anodes. The direction of K^+ movement reverses when PIBs supply power to an external circuit.

Anode materials for PIBs

This review focuses on the anode materials used in PIBs, and the mainstream materials are briefly summarized below. Significant efforts have been made to develop high-performance anode materials for

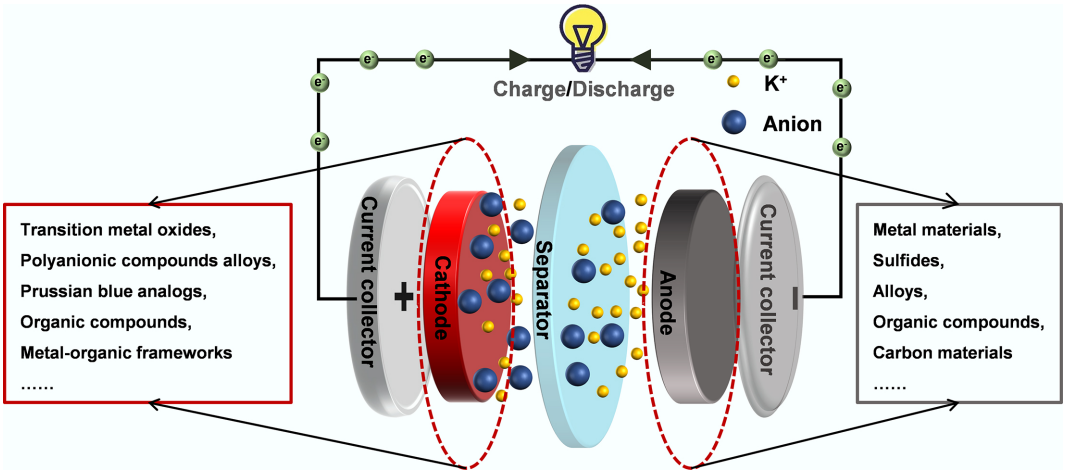

Fig. 1 Schematic illustration of the configuration and operational mechanism of a typical PIB.

PIBs, and a variety of materials have been successfully explored. Commonly used anode materials encompass metals, sulfides, alloys, organic compounds, and CMs[27].

The greatest advantage of metal anodes lies in their extremely high theoretical capacity[28]. For instance, the theoretical capacity of antimony metal is as high as 660 mAh g^{-1}[29]. However, due to the large volume of K^+, it is very hard for metals to recover to their original structures after several cycles of charging and discharging. Therefore, the capacity of PIBs with metal-based anode materials usually decreases very fast because of the complex phase change of metal oxides[30].

Sulfides, on the other hand, are attractive for their high voltage capabilities, while still maintaining an acceptable capacity[31]. However, sulfides undergo significant volume changes during cycling and are prone to side reactions, which leads to a short lifespan for PIBs with sulfides as anode materials.

The most well-known advantage of alloy anodes is their high capacity because of the synergistic effects between different metals[32]. However, as metal-based anodes, volume expansion of alloys during the cycles of charging and discharging is too obvious, which can lead to pulverization of the anode[33].

Organic materials, with their diverse and modifiable structures, can be tailored to meet specific requirements for batteries. Functional groups can be customized to provide user-defined voltage plateaus and storage capacities for various applications. However, the main challenges of organic materials as anode materials include poor electrical conductivity and low energy density. These limitations make the commercialization of PIBs with organic anodes a distant prospect[34].

For CMs, the most appealing factors are their mature and reliable commercial technology, with graphite having been widely produced. In addition, the ability of K^+ intercalation and deintercalation in CMs is remarkable, and the structure of CMs is generally stable[35]. Moreover, carbon materials also possess excellent chemical stability, mechanical strength, and thermal stability, making them arguably one of the most promising anode materials for PIBs.

BDCMs anode materials for PIBs

A high-performance anode requires excellent discharge capacity, rate performance, and cycling stability[36]. However, the large radius of K^+ leads to slow kinetics and structural instability in commercial anodes. Specifically, during the intercalation process, the larger size of K^+ causes slower kinetics and more significant expansion in commercial graphite anodes compared to Li^+. This, in turn, results in a decrease in rate performance and cycling stability. In contrast to commercial graphite, BDCMs exhibit a unique surface K^+ adsorption behavior, which is generally considered to enhance both rate performance and cycling stability in K^+ storage[37,38]. Therefore, current research is focused on improving the degree of disorder, morphology, and pore structure of BDCM anodes to enhance K^+ adsorption storage. As shown in Fig. 2, researchers have explored a variety of BDCMs as anode materials for PIBs. These include activated carbons (ACs), graphite-like carbons (GLCs), carbon aerogels (CAs), hard carbons (HCs), carbon dots (CDs), carbon nanotubes (CNTs), and carbon fibers (CFs), among others. Additionally, the corresponding preparation methods are also presented in Fig. 2. This section of the review primarily discusses the advantages and disadvantages of various BDCMs used as anode materials for PIBs. Furthermore, it highlights the research progress and the future prospects of BDCMs.

ACs

In the field of energy storage, ACs have attracted considerable attention owing to their well-developed porous structure and large specific surface area. These features endow ACs with abundant active sites, a broad electrode/electrolyte contact interface, and efficient K^+ transport[39].

Wang et al. prepared ACs from corn husk and KOH via a pyrolysis carbonization process at 800 °C for 2 h, targeting their use as anodes for PIBs; the preparation process is shown in Fig. 3a[40]. The mass ratios of KOH and corn husk are 1:2, 1:1, 2:1, and 4:1, and the corresponding samples were named AC-1, AC-2, AC-3, and AC-4. The SEM images presented in Fig. 3b–e show that the porosity improves significantly with increasing KOH content, which can be directly quantitatively verified with specific surface areas in Fig. 3f. Figure 3f indicates that the specific surface area of the ACs is strongly influenced by the ratio of KOH to corn husk during activation. Figure 3g, h demonstrates that the discharge capacity of the ACs is positively correlated with their BET specific surface areas. Among the four samples, AC-4, which has the largest specific surface area (1,760.3 m^2 g^{-1}), exhibits the highest discharge capacity throughout the entire cycling process at both 100 and 1,000 mA g^{-1}. This outstanding performance can be attributed to its large specific surface area and highly developed porosity, which provide extensive

https://doi.org/10.48130/scm-0026-0017

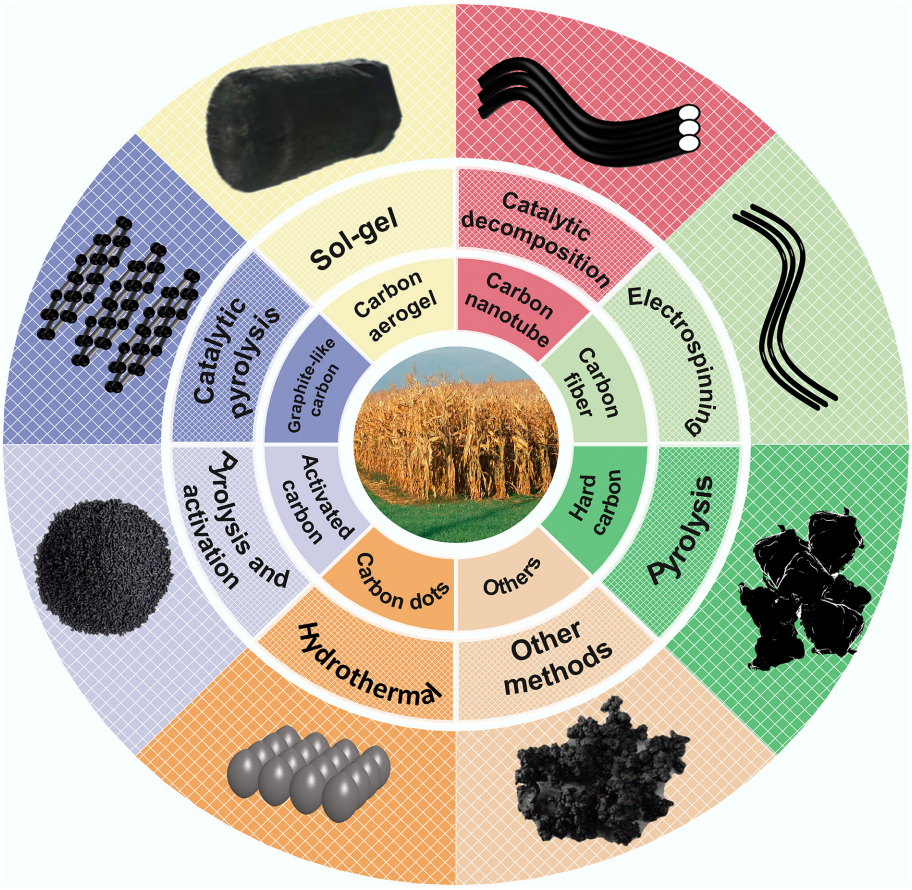

Fig. 2 Different BDCMs and one of their corresponding preparation methods.

interfaces between the electrode and electrolyte for efficient K^+ adsorption, diffusion, and storage[41]. Besides, such a large specific surface area promotes the formation of a stable solid electrolyte interphase (SEI) on the surface of the anode, which helps prevent further degradation during cycling[42].

While ACs with larger specific surface areas show promising potential for high discharge capacity as PIB anodes, their widespread use has been limited by poor cycling performance due to a low ion diffusion coefficient[43]. The electronic structure of ACs plays a crucial role in their cycling behavior. Doping heteroatoms, such as nitrogen, phosphorus, and sulfur, onto the surface of ACs can enhance their electronic structure, facilitating ion transport and improving cycling stability[44].

GLCs

Graphite has been widely used as a commercial anode material for LIBs due to its high stability as an intercalation compound[45]. In the case of PIBs, graphite also holds potential as an anode material due to its stable intercalation compound with high capacity[46]. However, the natural polymer structures of biomass contain abundant oxygen-containing functional groups, which make it challenging to fully graphitize biomass. Despite this limitation, these oxygen-containing functional groups are retained during the carbonization process, providing numerous active sites and resulting in a higher capacity compared to graphite anodes.

Figure 4a shows that Tang et al. conducted a study where Fe_2O_3/C particles were used for catalytic graphitization of tea-waste powder at 1,300 °C using a simple pyrolysis method to produce GLC[47]. The SEM image in Fig. 4b shows that GLC consists of micro-sized hollow tubes. Transmission electron microscopy (TEM) images in Fig. 4c, d reveal nano-sized graphitic crystals with numerous distinct and nearly parallel structures, further confirming the presence of graphite microcrystallites. The XRD curve in Fig. 4e shows a sharp diffraction peak at $2\theta = 26°$, corresponding to the graphite phase. As an anode for PIBs, the GLC anode achieves a high reversible specific capacity of 366 mAh g^{-1} after 200 cycles at 100 mA g^{-1} and a high initial ICE of 85.6%, as shown in Fig. 4f, g. Furthermore, in the long-term cycle test, the GLC anode retains 94% of its capacity after 1,000 cycles at 1,000 mA g^{-1}. The excellent electrical performance of GLC can be attributed to the large-sized graphitic domains, which are beneficial for reducing irreversible insertion sites, providing more diffusion channels for the intercalation/deintercalation of K^+ in the carbon interlayers, and shortening the diffusion distance. Additionally, the *in situ* XRD test result in Fig. 4i reveals the excellent reversible K^+ storage behavior of the highly crystalline structures in the GLC anode.

In the field of LIBs, the discovery and validation of stable intercalated compounds of LiC_6 have provided a direction for reducing the volume expansion of graphite anodes[48]. However, compared to LIBs, the GLC anode for PIBs exhibits a larger volume expansion, exceeding that of LIBs by more than 60%. This issue poses challenges to the lifetime and cycle capacity of PIBs. A series of intercalation compounds is formed in the storage process of potassium ions, such as KC_{24}, KC_{16}, KC_{10}, KC_8, KC, and so on, leading to a more complex potassiation reaction[49]. Therefore, investigating how to

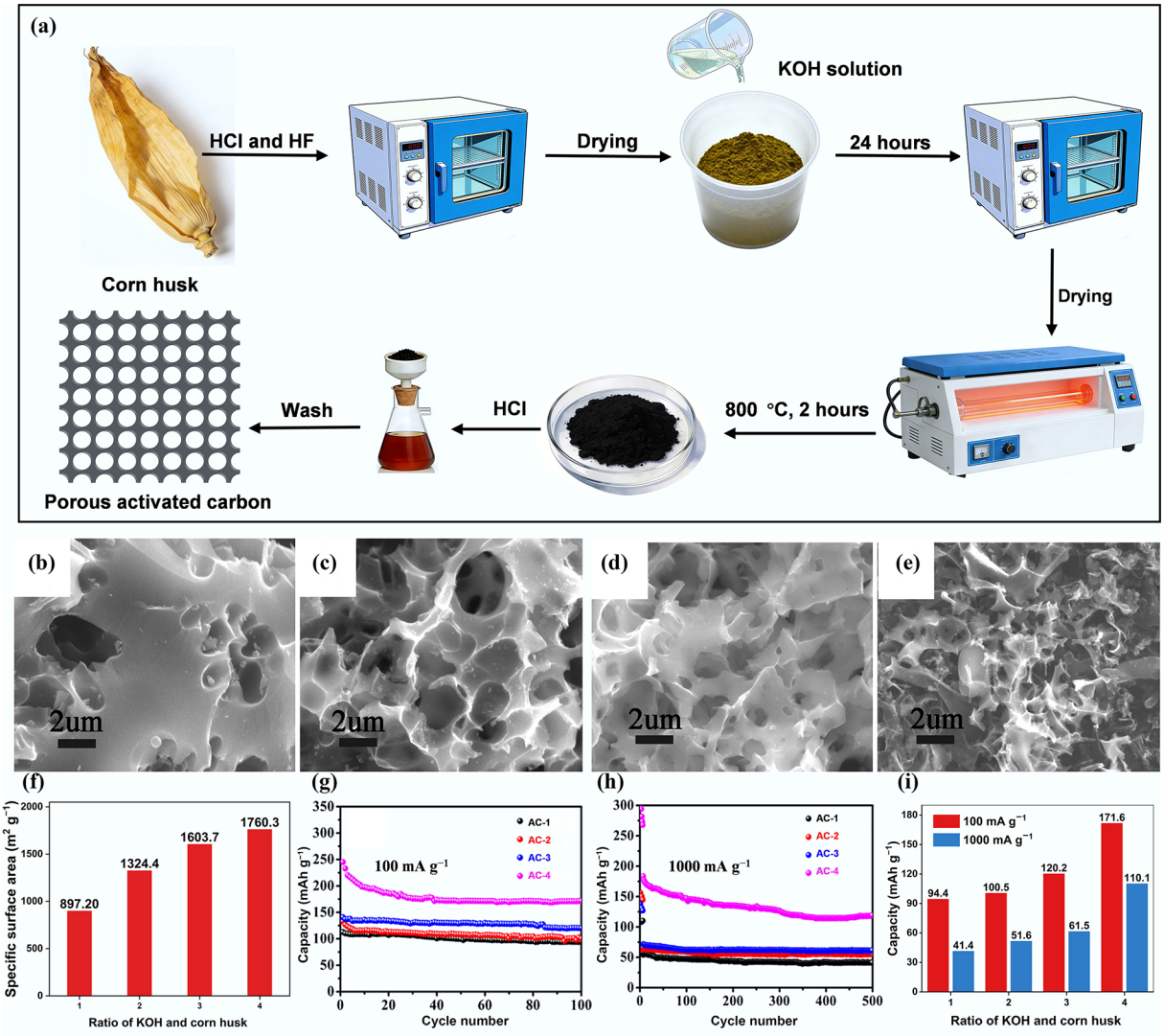

Fig. 3 (**a**) Schematic diagram of the preparation process of porous activated carbon from corn husk. SEM images of (**b**) AC-1, (**c**) AC-2, (**d**) AC-3, and (**e**) AC-4. (**f**) The effect of the ratio of KOH and corn husk on specific surface area; cycling performance of ACs at a current density of (**g**) 100 mA g^{-1} and (**h**) 1,000 mA g^{-1}. (**i**) The effect of the ratio of KOH and corn husk on the remaining capacity. Reproduced with permission[40]. Copyright 2019, Elsevier.

reduce the volume expansion of GLC anodes is key to improving potassium storage stability.

CAs

CA anodes exhibit key properties such as high porosity, large surface area, excellent conductivity, and good mechanical strength[50]. CAs are typically derived from biomass-based polysaccharides such as cellulose, starch, chitosan, and glycogen, which are valued for their widespread availability, renewability, and low toxicity[51,52]. Combined with their own intrinsic advantages and the merits of these raw materials, CAs are attractive anode materials for research on PIBs[53].

It has been reported that porous CAs can be produced from cellulose nanocrystals (CNCs) via an ice-templated method, and the specific synthetic procedures are shown in Fig. 5a[54]. A homogeneous suspension of CNCs mixed with polyethylene oxide (PEO) was freeze-dried under vacuum for 24 h at varying cooling rates of uncontrolled freezing, 3, 5, and 7 K min^{-1}. The resulting samples were then carbonized at 1,300 °C in a helium atmosphere for 2 h to produce the CAs, which were designated as VCA-U, VCA-3, VCA-5, and VCA-7. The SEM images (Fig. 5b–e) reveal that VCA-3, VCA-5, and VCA-7 exhibit smaller and more uniform cellular channels, as well as greater homogeneity, compared to VCA-U. Figure 5f shows that the lattice spacing decreases progressively while the defect density increases gradually. Among these, the VCA-5 anode demonstrates the best reversible capacity of 183 mAh g^{-1} and a capacity retention of 90.2% after 300 cycles at a rate of 0.5 C. The superior electrochemical performance of VCA-5 is attributed to its hollow channels, which shorten the K^+ diffusion pathway, while the enlarged interlayer spacing (0.39 nm) further promotes the intercalation and deintercalation of K^+. The results of potassium storage kinetics in Fig. 5i, j demonstrate that diffusion-controlled potassium storage is the primary potassium storage mechanism.

Although CAs have demonstrated outstanding electrochemical performance as anode materials for PIBs, their widespread application is still limited due to the challenges in their preparation process and the relatively low production yield[55]. The synthesis of biomass-derived CAs involves several complex steps, including mixing, stirring, sol-gel processing, and drying. These steps not only increase

https://doi.org/10.48130/scm-0026-0017

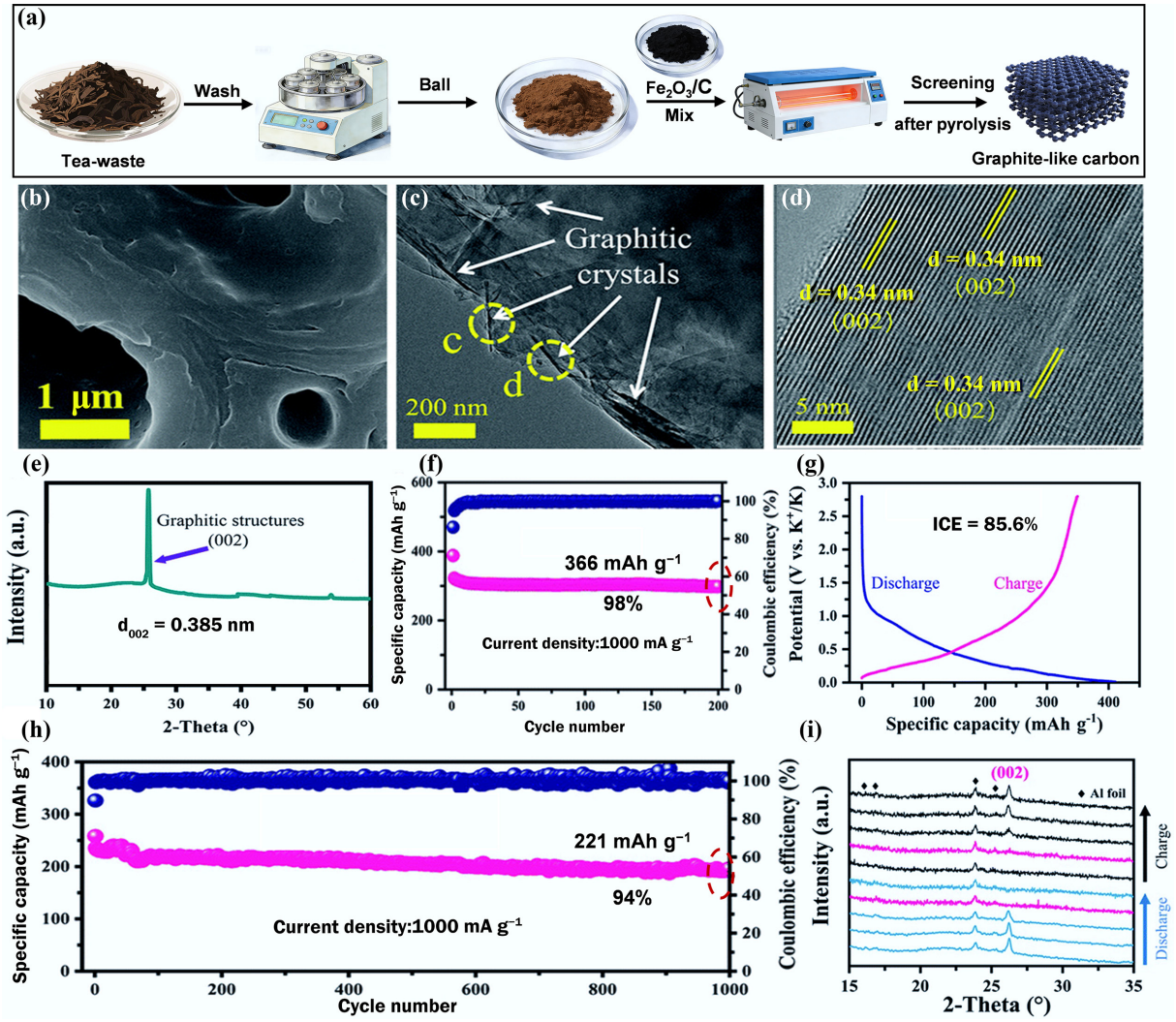

Fig. 4 (**a**) Schematic diagram of the catalytic synthesis of GLC from tea waste. (**b**) SEM. (**c**), (**d**) TEM images. (**e**) XRD curve. (**f**) Cycling performance. (**g**) Galvanostatic charge/discharge (GCD) curves at 100 mA g^{-1}. (**h**) Long-term cycling performance at 1,000 mA g^{-1}. (**i**) *In situ* XRD of GLC anode. Reproduced with permission[47]. Copyright 2021, Royal Society of Chemistry.

the complexity but also require considerable time, with the sol-gel phase alone taking between 24 and 48 h. To address these challenges, future research on CAs should focus on reducing the time and cost associated with their preparation.

HCs

HCs, a type of non-graphitic carbon material, have garnered increasing attention as anodes for PIBs owing to their high degree of structural disorder and excellent adsorption capacity. In the synthesis of HCs via biomass pyrolysis, the inherent randomness of the carbonization process disrupts both defect configurations and crystal ordering, resulting in a structure that remains difficult to graphitize even at elevated temperatures exceeding 2,500 °C[56]. These materials exhibit favorable electrochemical performance as PIB anodes, attributed to their high structural disorder, robust structural stability, and expanded graphite interlayer spacing[57].

In a study by Li et al., rice husk served as the precursor for HC synthesis via pyrolytic carbonization at varying temperatures (900, 1,100, 1,300, and 1,500 °C) for 2 h, with a heating rate of 5 °C min^{-1}, and the corresponding preparation process is illustrated in Fig. 6a[58]. The SEM and TEM images of HC carbonized at 1,300 °C (Fig. 6b–d) exhibit an irregular granular morphology; small pores are observable on its surface, which can shorten the pathway for potassium ion diffusion. In addition, random and disordered graphite microcrystals are observed, indicating the highly amorphous microstructure of HC. The characterization of structural properties revealed that the lattice spacing and defect density of HCs both decrease with increasing temperature (Fig. 6b). Figure 6c shows that the specific surface area and pore volume both decrease with increasing pyrolysis temperature. The cycling performance at a current density of 30 mA g^{-1} indicates that the discharge capacity of the rice husk-derived HC anodes first increased and then decreased with increasing pyrolysis temperature (Fig. 6d). Among all samples, HC carbonized at 1,300 °C delivered the highest discharge capacity over the entire cycling period, with a reversible capacity of 204.25 mAh g^{-1} after 100 cycles. Figure 6e illustrates that the best cycling performance of the HC carbonized at 1,300 °C stems from its highest adsorption contribution and good potassium ion diffusion coefficient, which is ascribed to its favorable defect structure (I_D/I_G = 1.38), appropriate specific surface area (83.3 m^2 g^{-1}), and large d_{002} value (0.378 nm).

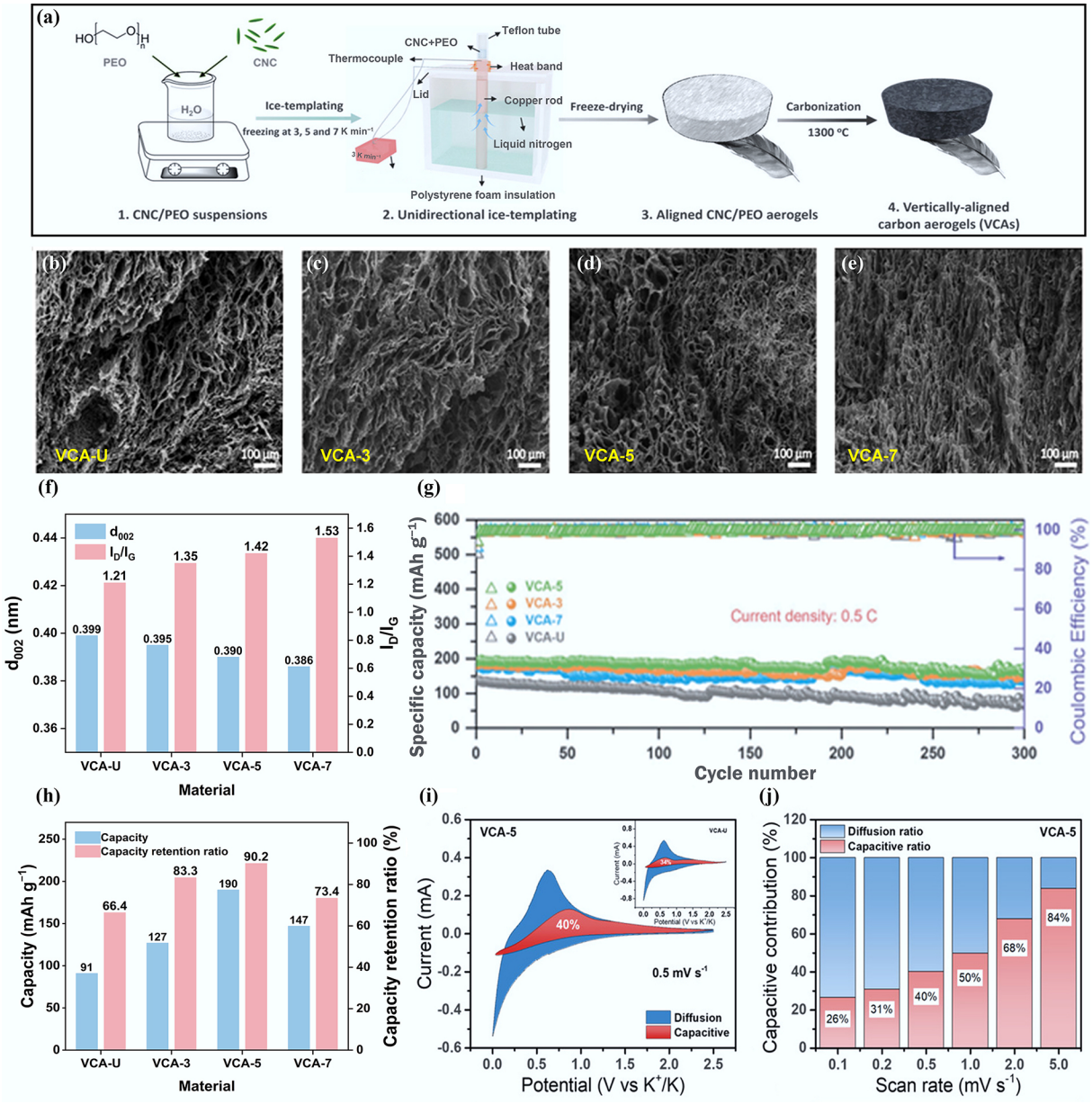

Fig. 5 (**a**) Synthesis process of CNC-derived CAs. (**b**)–(**e**) SEM images of CAs. (**f**) Structural properties. (**g**) Cycling performance at a current density of 0.5 C. (**h**) The capacity and capacity retention ratio of four anodes. (**i**) Separation of the capacitive and diffusion-controlled charges at 0.5 mV s^{-1}. (**j**) Contribution ratios of the capacitive and diffusion-controlled charge at various scan rates. Reproduced with permission[54]. Copyright 2022, Wiley-VCH.

Despite significant progress in the development of HC anodes for PIBs, several challenges remain to be addressed before their commercialization. The relatively low initial coulombic efficiency (ICE) and specific capacity are the primary factors impeding the practical application of HCs as PIB anodes[59]. Enhancing both ICE and specific capacity is therefore a key research goal for the development of high-energy-density PIBs. Furthermore, significant controversy persists regarding the K^+ storage mechanism of HC anodes for PIBs. It is widely accepted that both the intercalation and adsorption mechanisms play major roles in potassium storage. However, the existence of a 'filling' mechanism remains a topic of debate due to the lack of advanced *in situ* characterization, which has resulted in an absence of direct evidence[60]. Moreover, because of the highly disordered structure of biomass-derived hard carbon materials, these materials typically exhibit a high proportion of adsorption capability. Consequently, no distinct discharge plateau is observed in their GCD curves, while a broad peak tends to emerge during the potassium deintercalation process in their CV curves[61]. This variability makes it challenging to delineate the boundary between the adsorption and intercalation sites. Additional experimental and theoretical evidence is required to thoroughly investigate these storage mechanisms and achieve a more comprehensive understanding of the underlying processes.

CNTs

CNTs have emerged as promising anode materials for PIBs due to their several desirable characteristics, including high conductivity, low density, high strength, and unique structural properties. One of the

https://doi.org/10.48130/scm-0026-0017

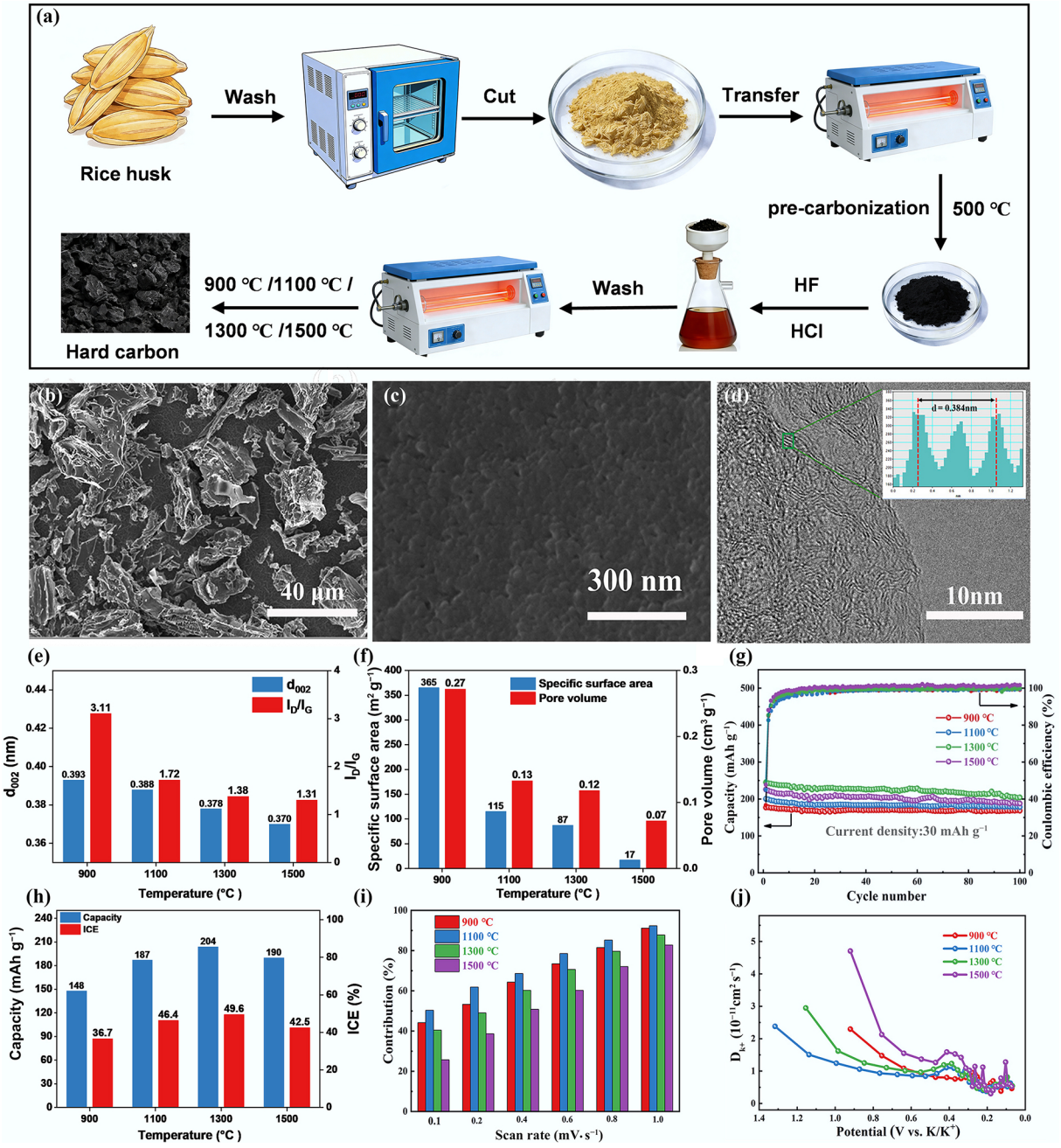

Fig. 6 (**a**) Preparation process of rice husk-based HCs. (**b**), (**c**) SEM. (**d**) TEM images of HC carbonized at 1,300 °C. (**e**) Structural properties of HCs. (**f**) Pore property. (**g**) Cycling performance of HCs at a current density of 30 mA g^{-1}. (**h**) The effect of pyrolysis temperature on the capacity and ICE. (**i**) The contribution of the capacitance at different scan rates. (**j**) Diffusion coefficients of the discharge process. Reproduced with permission[58]. Copyright 2020, Elsevier.

advantages of CNTs is their ability to function as independent anode materials without the need for binders or conductive additives. This is attributed to the interconnected conductive network formed by the CNTs themselves[62,63]. Moreover, the absence of dead volume materials in CNT-based anodes helps to mitigate volume expansion during cycling, thereby improving the cycling life of PIBs[64]. Various synthesis methods are available for CNT production, including chemical vapor deposition (CVD), catalytic pyrolysis, solvothermal methods, and hydrothermal methods[65]. These methods allow for the control of physicochemical properties such as specific surface area and crystallinity according to specific requirements.

It has been reported that the Fe_3C-embedded CNTs (Fe_3C@CNTs) were synthesized using distilled grains as the raw material in the presence of melamine (nitrogen source) and $FeCl_3/ZnCl_2$ activators (Fig.7a)[66]. SEM images of Fe_3C@CNT revealed a fibrous structure with a hollow interior, and TEM images showed the presence of Fe_3C nanoparticles within the CNTs. The hollow structure of Fe_3C@CNT serves as an efficient ion transport channel, facilitating the rapid intercalation/deintercalation of potassium ions during battery operation. Consequently, as shown in Fig. 7f–h, Fe_3C@CNT shows a low ICE with 55% but excellent cycling performance with a capacity of

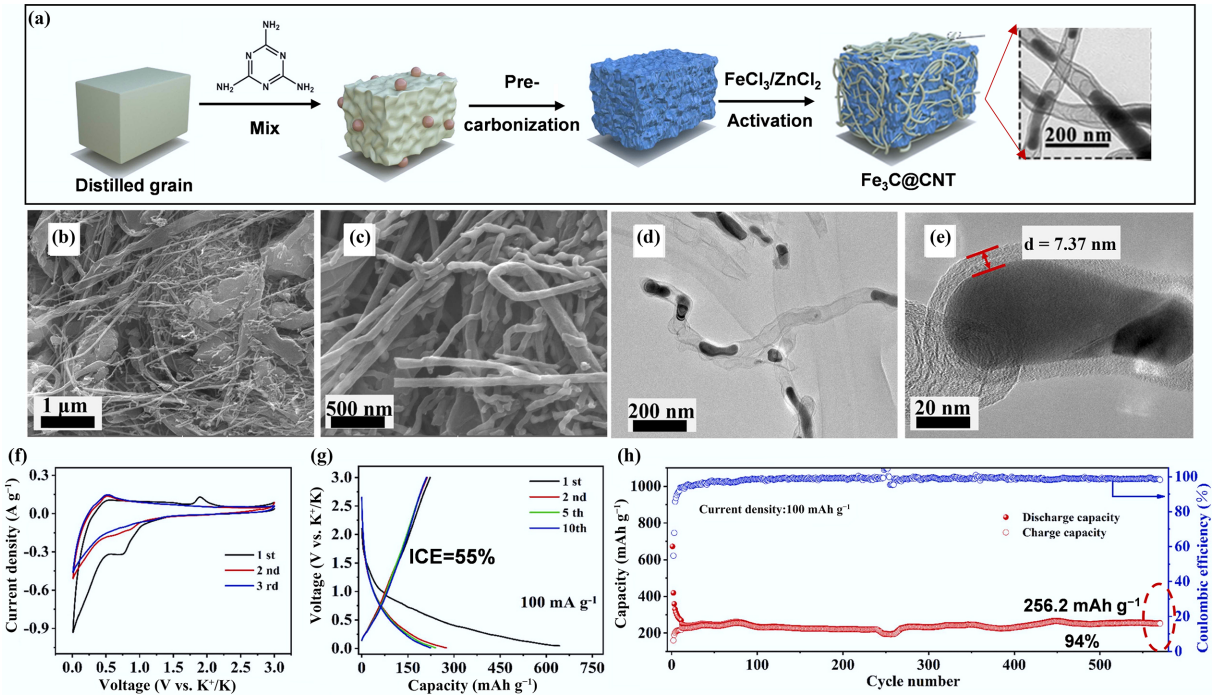

Fig. 7 (**a**) Schematic of Fe_3C@CNT synthetic process. (**b**), (**c**) SEM images. (**d**), (**e**) TEM images. (**f**) CV profiles at a scan rate of 0.2 mV s^{-1}. (**g**) GCD curves. (**h**) Cycling performance in PIBs at a current density of 100 mA g^{-1}. Reproduced with permission[66]. Copyright 2022, Elsevier.

256.2 mAh g^{-1} and a high capacity retention ratio of 94% after 600 cycles at a current density of 100 mA g^{-1}.

CNTs possess superior electrochemical and structural properties compared to most other BDCMs, making them ideal anode materials for PIBs without the need for additional binders or conductors. However, the main challenge lies in the limited availability of high-quality CNTs, which hampers mass production. Furthermore, the physicochemical properties of CNTs can vary significantly depending on the biomass used for their synthesis[67]. Different biomass sources have different compositions, resulting in variations in the properties of the resulting CNTs. Mathangi et al. prepared CNTs from *Citrullus lanatus* rind, *Gleditsia triacanthos* pod, *Cocos nucifera* exocarp, and *Prosopis juliflora* wood using a hydrothermal method, as illustrated in Fig. 8[68]. Significant differences in the (002) crystal plane indicate variations in their crystal lattices. The differences in peak positions and intensities observed in Raman spectroscopy reveal the structural distinctions, which in turn affect electrical conductivity and the degree of graphitization. Scanning Electron Microscopy (SEM) images provide a clear visual representation of the differences in CNTs synthesized from different raw materials, including variations in tube diameter, length, and uniformity. Additionally, using a single component such as cellulose as a raw material may increase the preparation cost of CNTs. To address the issue of supply shortage, it would be beneficial to identify biomass sources with larger storage capabilities that can be used for CNT synthesis. By selecting appropriate biomass materials, high-quality and high-yield CNTs can be produced to meet the demand for anode materials in PIBs.

CDs

CDs are a class of carbon nanomaterials that are small in size and rich in functional groups, such as –COOH, –OH, $–NH_2$, etc. From the perspective of structure and composition, they are a kind of transition material between organic molecules and inorganic carbon materials[69]. The abundant surface functional groups can serve as suitable adsorption sites for K^+ storage, while the ultrasmall size can provide high utilization efficiency, fully expose reaction sites, and be used for K^+ storage. Therefore, CDs have been demonstrated to have huge potential in the field of energy storage systems owing to their many characteristics and advantages.

One notable study by Wang et al. synthesized nano CDs from soybean via a strategy involving hydrothermal treatment followed by pyrolysis and the sacrificial template method, as shown in Fig. 9a[70]. The SEM and TEM images in Fig. 9b–d reveal that the material exhibits alveolate porous structures and highly disordered carbon layer structures. The XRD curve in Fig. 9e shows the disordered structure, while the abundant nitrogen- and oxygen-containing functional groups are revealed by Fourier transform-infrared spectroscopy (FT-IR) in Fig. 9f. Figure 9g, h show the CD anode retains 234.5 mAh g^{-1} after 200 cycles at 100 mA g^{-1} and even 152.0 mAh g^{-1} after 1,000 cycles at a current density of 1,000 mA g^{-1}. The kinetic analysis (Fig. 9i) shows that the good K^+ storage performance is attributed to its high adsorption capacity, owing to its abundant surface functional groups.

Although CDs currently exhibit good electrochemical performance and their synthesis process is relatively simple, their high adsorption capacity simultaneously leads to low ICE and a relatively high operating voltage. Therefore, the energy density is not ideal in the assembly of full cells. Drawing on lessons from LIBs and SIBs, pre-filling with lithium and sodium—i.e., pre-lithiation and pre-sodiation—is a highly straightforward and efficient method to obtain high ICE of CD anodes[71]. Therefore, a pre-potassiation strategy can be applied to CD anodes to improve the ICE and thereby achieve higher energy density in PIBs.

https://doi.org/10.48130/scm-0026-0017

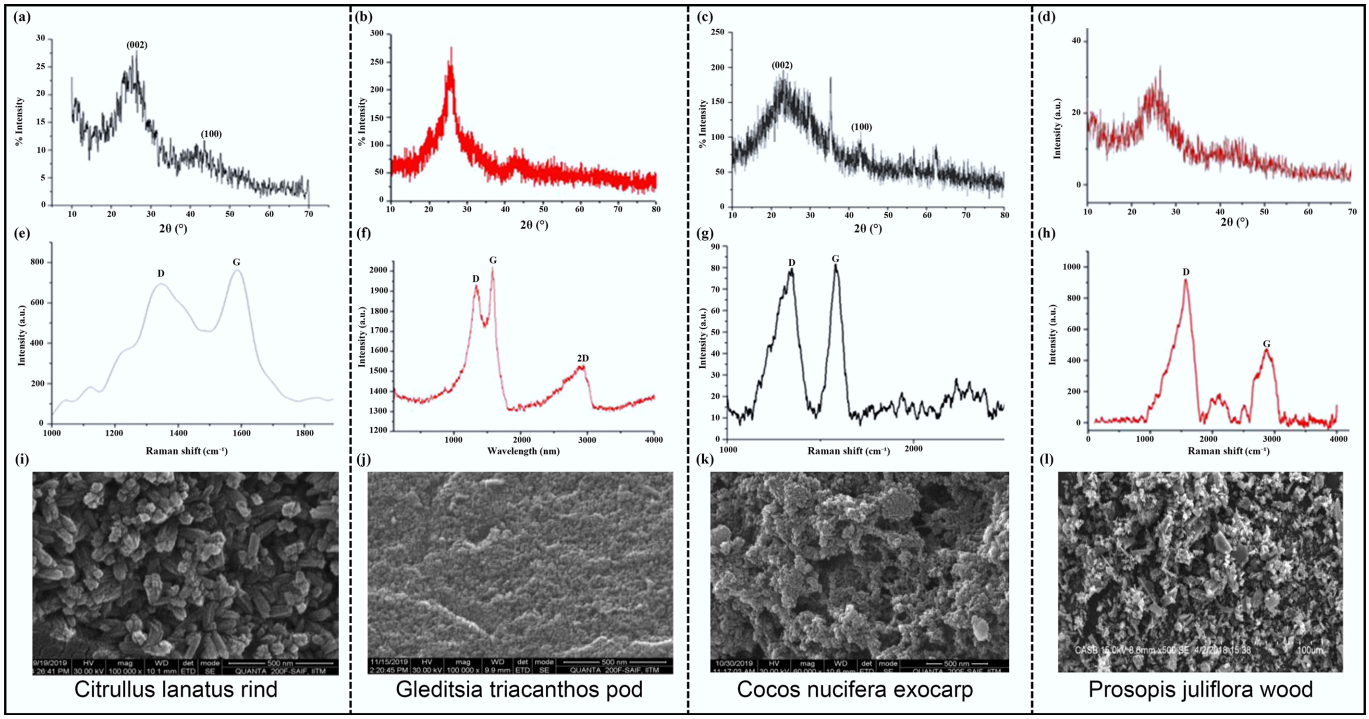

Fig. 8 (**a**)–(**d**) XRD curves. (**e**)–(**h**) Raman spectra. (**i**)–(**l**) SEM images of CNTs derived from *Citrullus lanatus* rind, *Gleditsia triacanthos* pod, *Cocos nucifera* exocarp, and *Prosopis juliflora* wood[68]. Copyright 2020, Taylor & Francis.

CFs

CFs possess a unique combination of high mechanical strength, flexibility, and excellent electrical conductivity, rendering them suitable for energy storage applications[72]. The increasing demand for efficient energy storage and conversion devices has led to a significant boost in CFs production and development[73]. Various techniques, such as wet-spinning, dry-spinning, melt-spinning, and electrospinning, have been employed to synthesize CFs from biomass sources, with lignocellulosic materials being one of the most popular raw material choices[74,75].

Jiang et al. used bovine hide as a precursor material for the synthesis of N-doped CFs (Fe_2N@N-CFBs)[76]. The synthetic process, as depicted in Fig. 10a, utilized $Fe_2(SO_4)_3$ and NH_3 as precursors for Fe and N, respectively, via a pyrolysis carbonization method. XRD analysis in Fig. 10b revealed three prominent characteristic peaks at 40.9°, 42.9°, and 56.7°, indicating the presence of Fe_2N in Fe_2N@N-CFBs. The Raman spectrum analysis revealed an I_D/I_G ratio of 1.12 for Fe_2N@N-CFBs, suggesting the presence of a large number of defects and a highly disordered structure within the CFs. SEM images in Fig. 10d, e displayed the fibrous structure of Fe_2N@N-CFBs. Figure 10f demonstrates that the rate performance and reversible discharge capacity of the Fe_2N@N-CFBs anode significantly improved compared to those of bare Fe_2N nanofibers (Fe_2N-FBs). As illustrated in Fig. 10g, the reversible capacity of Fe_2N@N-CFBs anode materials decreased to 102 mAh g^{-1} after 100 cycles, while maintaining a coulombic efficiency close to 100%. In contrast, Fe_2N-FBs showed a reversible capacity of only 64 mAh g^{-1} in the first cycle, which further declined to a nearly negligible level of 22 mAh g^{-1} in the last cycle. This comparison highlights that the introduction of N can enhance the conversion kinetics of CFs, ultimately improving their electrochemical performance as anodes for PIBs.

Although biomass-derived CFs have the advantages of environmental friendliness, renewability, and low cost, their discharge capacity in PIBs is low, and the conductivity of pure CFs is much lower than that of graphite due to their low graphitization. These problems limit the application of CFs[77]. It is possible that preparing hollow porous CFs and increasing the graphitization degree of CFs can significantly improve the electrochemical performance in PIBs. The electrochemical performance of biomass-derived CFs can also be improved by incorporating other active precursor materials, such as metal salt, nitride, etc., during the synthesis process[78].

Preparation methods of BDCMs

Carbonization methods

The carbonization process is a necessary step from biomass to carbon, regardless of the type of CMs. Common carbonization methods include pyrolysis, hydrothermal, and microwave-assisted processes. Additionally, there have been explorations into novel thermal carbonization techniques such as plasma-enhanced chemical vapor deposition, Joule heating, and laser scribing and writing methods[79,80]. However, the complicated production processes and high costs associated with these novel techniques have limited their widespread application; therefore, these methods are not reviewed here. Consequently, this section focuses on introducing pyrolytic carbonization, hydrothermal carbonization, and microwave carbonization. As shown in Fig. 11, their respective influencing factors, advantages, and disadvantages are presented.

Introduction of common carbonization methods

Pyrolysis carbonization is a thermochemical decomposition process of biomass conducted under inert gas protection and high temperatures. In addition to CMs, the products of biomass pyrolysis include biofuels and biogases[81]. Factors, including heating rate, pyrolysis time, and final temperature, have a significant effect on the morphology, porosity, degree of disorder, and lattice spacing of BDCMs[82]. Pyrolysis methods can be widely used for various biomass sources to produce

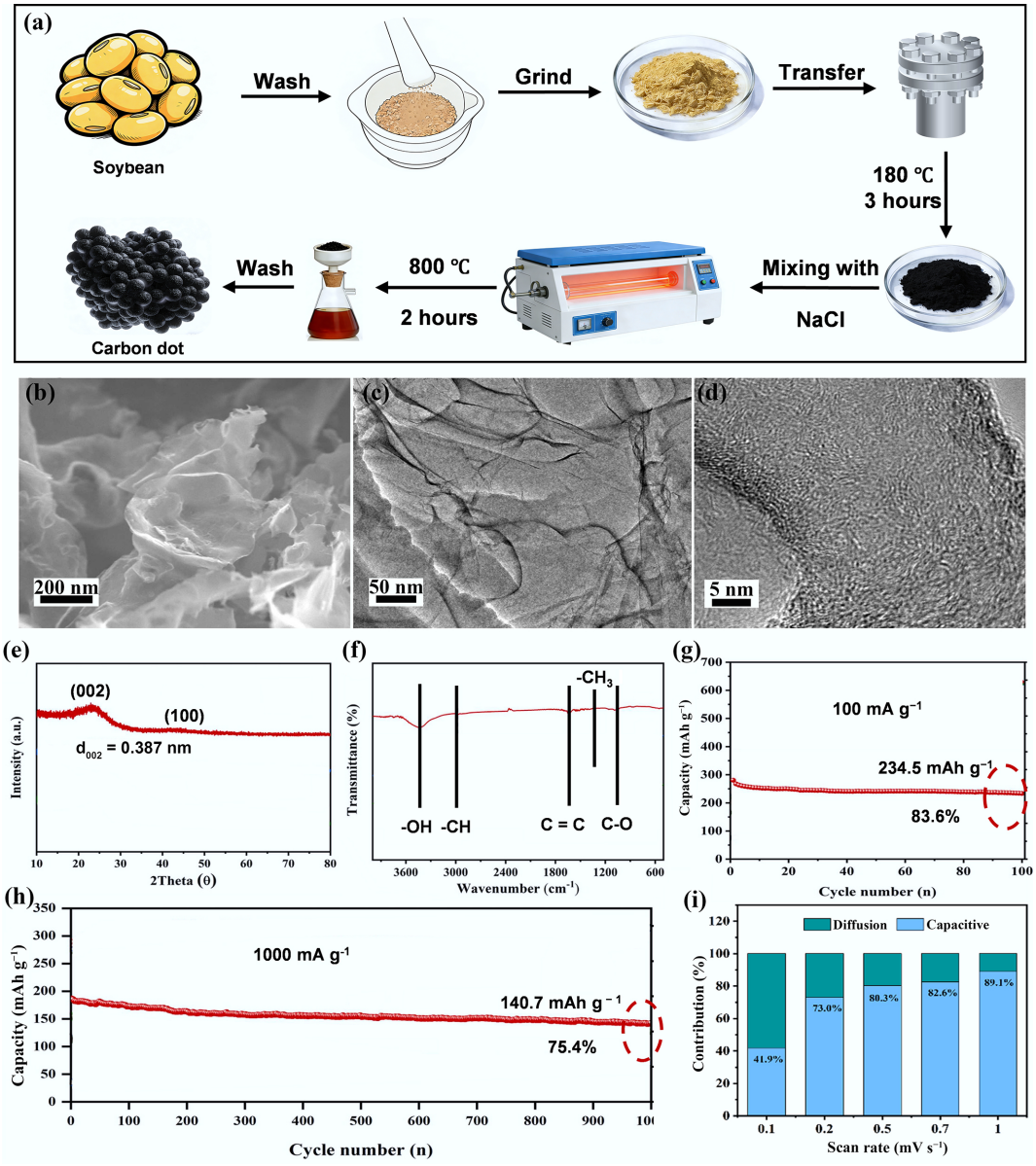

Fig. 9 (**a**) Synthetic process from soybean to CDs. (**b**) SEM images. (**c**), (**d**) TEM images. (**e**) XRD curve. (**f**) FT-IR. (**g**) Cycling performance at a current density of 100 mA g^{-1}. (**h**) long cycling performance at a high current density of 1,000 mA g^{-1}. (**i**) K^+ storage performance kinetic analysis. Reproduced with permission[70]. Copyright 2022, Elsevier.

BDCM anodes with high yield for PIBs, including ACs, GLCs, HCs, and others[83]. However, in large-scale production, uneven heating and high energy consumption are intractable key issues.

Hydrothermal carbonization is a process that converts biomass into carbon materials in a sealed container under high temperatures (180–250 °C) and pressures (2–10 MPa)[84]. Several factors can influence the size and morphology of BDCMs prepared by hydrothermal carbonization, including the concentration of the raw material, solvent, pH, and pressure[85]. Compared with pyrolysis biochar, hydrochar has a lower carbonization degree, which indicates the lower thermal stability; therefore, hydrochar usually cannot be directly used as anodes for PIBs[86]. However, abundant oxygen-containing groups and a high degree of disorder make hydrochar suitable for the reversible intercalation and de-intercalation of larger-sized potassium ions[87]. To obtain BDCMs with a high carbonization degree, hydrothermal carbonization should be further treated to prepare high-performance anodes for PIBs.

Microwave carbonization achieves the carbonization of biomass by promoting internal molecular interactions within the biomass, thereby generating heat and inducing the carbonization process[88]. This process has been regarded as an alternative to conventional pyrolysis. Microwave power, microwave frequency, and the microwave absorption capacity of biomass all significantly affect the carbonization process and the characteristics of the resulting BDCMs. Microwave carbonization has the advantages of rapid heating rates and uniform heating, which can improve reaction rates and energy efficiency. Biomass requires drying before conventional pyrolysis carbonization, but it can be utilized directly in microwave carbonization. In addition, microwave-assisted pyrolysis can achieve instantaneous heating of feedstock by allowing for an instant on/off

https://doi.org/10.48130/scm-0026-0017

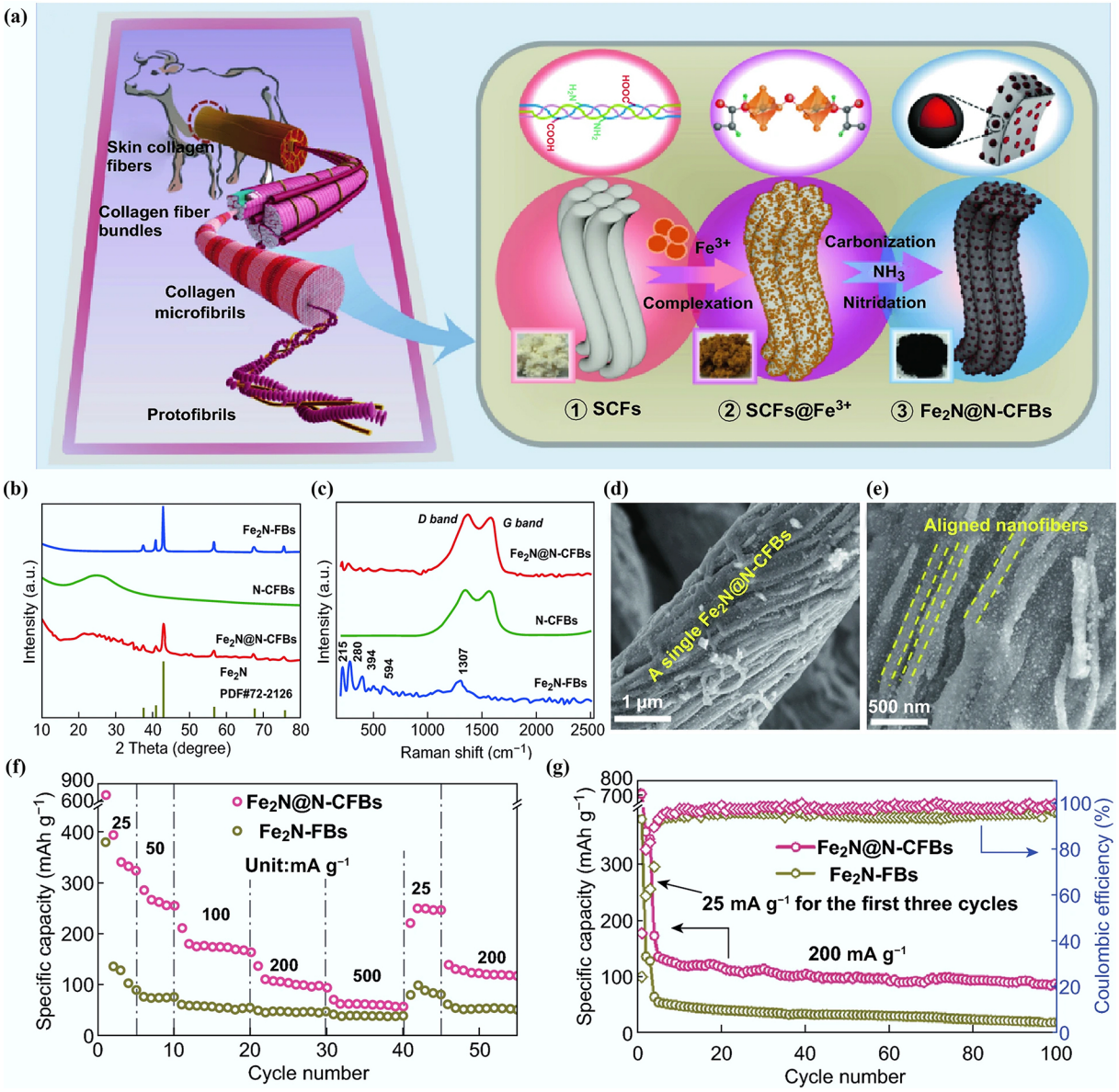

Fig. 10 (**a**) Synthetic process from bovine hide to Fe_2N@N-CFB. (**b**) XRD patterns. (**c**) Raman spectra. (**d**), (**e**) SEM images. (**f**) Rate performance. (**g**) Cycling performance for 100 cycles at 200 mA g^{-1}. Reproduced with permission[76]. Copyright 2019, Springer Nature.

control, reducing the impact of heat transfer. Moreover, the microwave method not only simplifies operation but also increases product quality[89,90]. The pronounced selectivity of microwave heating primarily arises from variations in dielectric constants among different biomass materials. These variations stem from differences in ash content, oxygen-containing functional groups, particle size, and moisture content, all of which influence the efficiency of microwave carbonization. To address this challenge, several strategies have been reported in the literature[91]. One effective approach involves the use of microwave absorbers to enhance the dielectric properties of biomass. By adjusting the dosage of such additives, the dielectric constants of different biomass feedstocks can be tuned to comparable levels. For instance, Mattia et al. added silicon carbide as a microwave absorber to olive tree pruning residues[92]. This addition enabled the system temperature to reach 700 °C within 21 min, yielding BDCMs at a rate as high as 60%.

Comparison of carbonization methods

As Fig. 11 shows, the carbonization methods mentioned above provide insights into the preparation of BDCMs for practical applications, and different approaches have their own advantages and disadvantages. Slow pyrolysis is one of the most popular carbonization methods for converting biomass into various BDCMs, whose specific surface area is relatively large, and the reaction time of carbonization is shorter than that of the hydrothermal carbonization method. However, the biochar from biomass pyrolysis usually cannot be directly used as anodes for PIBs; therefore, further activation is necessary, and pretreatment of biomass before pyrolysis is also an effective way to obtain high-quality BDCMs. Compared with pyrolysis, hydrothermal carbonization exhibits lower energy consumption and better morphological control of the resulting hydrochar; however, its poor porosity necessitates additional activation processes. Different from conventional pyrolysis, the heating rate of microwave-assisted pyrolysis is usually faster, and pretreatment, such as drying, can be omitted. However, raw

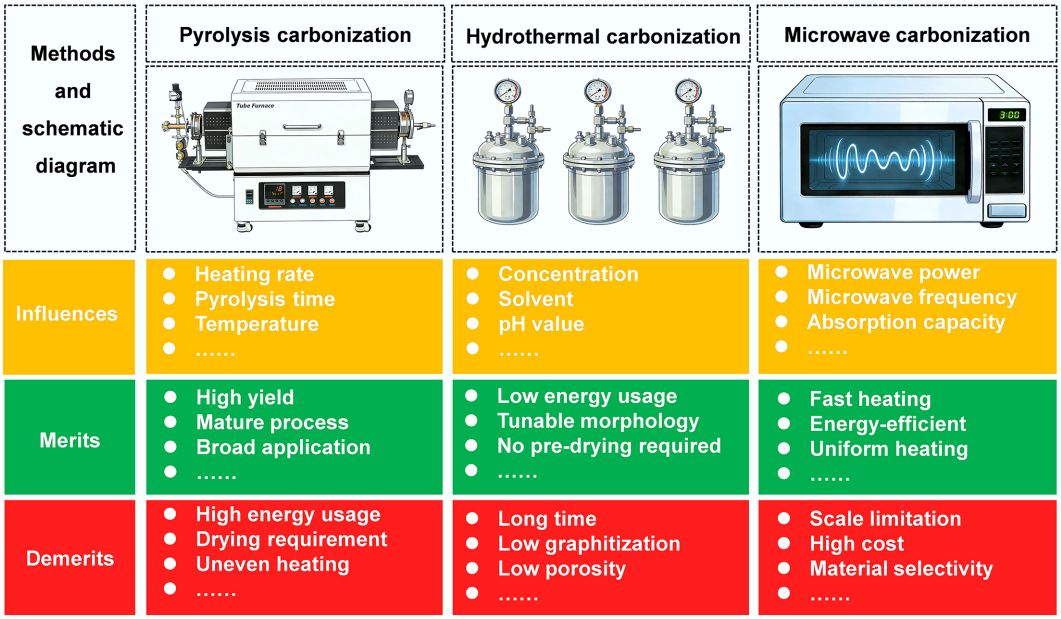

Fig. 11 Main carbonization methods, their influencing factors, merits, and demerits.

materials often require additional microwave absorbents, and economic feasibility remains uncertain for future applications[93].

Activation methods

BDCMs prepared by direct carbonization often exhibit an unfavorable pore structure and cannot be directly used for potassium storage; therefore, they require further modification. Activation is the most effective approach to prepare porous BDCMs, including chemical activation and physical activation. Both approaches can improve the pore structure and morphological characteristics of BDCMs, thereby increasing potassium ion adsorption properties.

Physical activation

Physical activation is generally conducted in the presence of oxidizing gases, primarily including air, steam, or CO_2. These gases remove the residual products in the char pores through gasification reactions within a temperature range of 350–1,000 °C, during which closed pores can be opened. Then, more porous structures and improved potassium ion adsorption properties can be achieved via complex reactions. Among common activation gases, CO_2 has been the most widely used to activate char due to its low price, easy availability, and abundance. In addition, CO_2 can etch the char and develop porous structures within the carbon skeleton[94]. Viewed from the whole process, the two greatest advantages of physical activation are the absence of environmental pollution and a simple production process; however, high energy consumption and long activation time are the main factors that restrict the wide application of physical activation methods.

Chemical activation

Chemical activation is the main method for preparing porous BDCMs. Many chemicals can serve as activating agents of chemical activation, including H_3PO_4, KOH, NaOH, K_2CO_3, $ZnCl_2$, and others[95]. In addition to creating abundant pore structures, chemical activators can etch the carbon surface to make it rough, which is beneficial for potassium ion storage. However, excessive activators can cause pore collapse, leading to a decrease in specific surface area and consequently a decline in the electrochemical performance of BDCM anodes[96]. Although chemical activation is a widely used method for producing BDCMs, it often involves harsh reagents that require extensive post-treatment, corrode equipment, and pose environmental risks[97]. Thus, the development of environmentally friendly activators is essential to ensure both effective activation and ecological sustainability. For example, Muhammad et al. used sodium oxalate as a green activator in the co-pyrolysis of date seed powder. Upon heating to approximately 500 °C, sodium oxalate decomposes into sodium carbonate. As the temperature increases to around 700 °C, sodium carbonate further decomposes to produce sodium oxide and carbon dioxide. At 800 °C, sodium oxide breaks down into metallic sodium and carbon monoxide, while carbon dioxide is simultaneously reduced by carbon in the system. These reactions promote carbon gasification, thereby significantly increasing the porosity. Metallic sodium plays a critical role by intercalating into the carbon matrix, inducing lattice distortion and swelling. Although subsequent water washing removes the sodium, the altered carbon structure remains, resulting in a unique porous microstructure.

Conclusions and future perspectives

In summary, this review systematically summarizes different BDCM anodes for potassium storage, discusses their respective advantages, identifies existing challenges, and proposes several future research directions along with corresponding solutions: optimizing the surface electronic structure of ACs, for instance, through heteroatom doping, can enhance cycling performance. Balancing the adsorption/intercalation behavior of K^+ in GLCs or HCs provides a viable strategy to mitigate volume expansion. Furthermore, pre-potassiation is an effective approach to improve the initial ICE of HCs and CDs, thereby enabling high-energy-density PIBs. In terms of CAs, high cost is a major factor limiting their large-scale application. Additionally, complex preparation processes and prolonged synthesis times are pressing issues that require urgent resolution. CNTs exhibit nearly ideal performance as PIB anode materials, with the only constraint being limited supply. Thus, selecting appropriate biomass precursors with abundant reserves represents an efficient solution to this problem. Future research on CFs should prioritize enhancing their porosity

and graphitization degree. Moreover, carbonization and activation methods significantly affect the morphology and electrochemical performance of BDCMs, highlighting the need for greater attention to the development of optimized preparation processes. Overall, this review summarizes recent advances in different BDCM anodes for PIBs. It is anticipated to serve as a valuable reference for researchers designing advanced carbon-based anodes with excellent K^+ storage capabilities for PIBs.

Author contributions

The authors confirm their contributions to the paper as follows: study conception, design, and draft manuscript preparation were performed by Yongfeng Zhu; data collection was performed by Xiaowen Liu; review & editing were performed by Jinze Dai and Qingang Xiong; funding acquisition was performed by Xiaowen Liu and Qingang Xiong. All authors reviewed the results and approved the final version of the manuscript.

Data availability

The datasets used or analyzed during the current study are available from the corresponding author upon reasonable request.

Funding

This work was supported by the National Natural Science Foundation of China (Grant No. 22208109), and the National Key R&D Project of China (Grant No. 2023YFD2201902).

Declarations

Conflicts of interests

The authors declare that they have no conflict of interest.

Author details

State Key Laboratory of Pulp and Paper Engineering, School of Light Industry and Engineering, South China University of Technology, Guangzhou 510641, China

References

[1] Xia M, Zhou J, Lu B. 2025. Comprehensive insights into aqueous potassium-ion batteries. *Advanced Energy Materials* 15:2404032

[2] Xia M, Fu H, Lin K, Rao AM, Cha L, et al. 2024. Hydrogen-bond regulation in organic/aqueous hybrid electrolyte for safe and high-voltage K-ion batteries. *Energy & Environmental Science* 17:1255–1265

[3] Luo Y, Mou P, Yuan W, Li L, Fan Y, et al. 2023. Anti-liquid metal permeation separator for stretchable potassium metal batteries. *Chemical Engineering Journal* 452:139157

[4] Sha M, Liu L, Zhao H, Lei Y. 2020. Review on recent advances of cathode materials for potassium-ion batteries. *Energy & Environmental Materials* 3:56–66

[5] Liu H, Cheng XB, Jin Z, Zhang R, Wang G, et al. 2019. Recent advances in understanding dendrite growth on alkali metal anodes. *EnergyChem* 1:100003

[6] Li Y, Kabanova NA, Blatov VA, Wang J. 2025. High-throughput screening of phosphide compounds for potassium-ion conductive cathode application. *Journal of Materials Informatics* 5:21

[7] Guo X, Xie H, Kumar P, Liang H, Zhao F, et al. 2025. High-rate, long-lifespan, sustainable potassium-ion batteries enabled by non-fluorinated solvents. *Materials Science and Engineering: R: Reports* 166:101063

[8] Xu YS, Duan SY, Sun YG, Bin DS, Tao XS, et al. 2019. Recent developments in electrode materials for potassium-ion batteries. *Journal of Materials Chemistry A* 7:4334–4352

[9] Zhang J, Liu T, Cheng X, Xia M, Zheng R, et al. 2019. Development status and future prospect of non-aqueous potassium ion batteries for large scale energy storage. *Nano Energy* 60:340–361

[10] Okoshi M, Yamada Y, Komaba S, Yamada A, Nakai H. 2017. Theoretical analysis of interactions between potassium ions and organic electrolyte solvents: a comparison with lithium, sodium, and magnesium ions. *Journal of the Electrochemical Society* 164:A54–A60

[11] Komaba S, Hasegawa T, Dahbi M, Kubota K. 2015. Potassium intercalation into graphite to realize high-voltage/high-power potassium-ion batteries and potassium-ion capacitors. *Electrochemistry Communications* 60:172–175

[12] Wu X, Leonard DP, Ji X. 2017. Emerging non-aqueous potassium-ion batteries: challenges and opportunities. *Chemistry of Materials* 29:5031–5042

[13] Zhou M, Bai P, Ji X, Yang J, Wang C, et al. 2021. Electrolytes and interphases in potassium ion batteries. *Advanced Materials* 33:2003741

[14] Liu Y, Gao C, Dai L, Deng Q, Wang L, et al. 2020. The features and progress of electrolyte for potassium ion batteries. *Small* 16:2004096

[15] Eftekhari A, Jian Z, Ji X. 2017. Potassium secondary batteries. *ACS Applied Materials & Interfaces* 9:4404–4419

[16] Yang M, Dai J, He M, Duan T, Yao W. 2020. Biomass-derived carbon from *Ganoderma lucidum* spore as a promising anode material for rapid potassium-ion storage. *Journal of Colloid and Interface Science* 567:256–263

[17] Cui L, Wang Z, Kang S, Fang Y, Chen Y, et al. 2022. N, P codoped hollow carbon nanospheres decorated with $MoSe_2$ ultrathin nanosheets for efficient potassium-ion storage. *ACS Applied Materials & Interfaces* 14:12551–12561

[18] Wu X, Chen Y, Xing Z, Lam CWK, Pang SS, et al. 2019. Advanced carbon-based anodes for potassium-ion batteries. *Advanced Energy Materials* 9:1900343

[19] Li M, Wang C, Wang C, Lyu Y, Wang J, et al. 2025. 10 years development of potassium-ion batteries. *Advanced Materials* 37:2416717

[20] Mao Z, Wang H, Zhang T, Wang Y, Zhou W, et al. 2025. Synergetic electrolyte chemistry enables flame-retardancy, K^+-desolvation, anti-corrosion and wide-temperature-tolerance in potassium-ion batteries. *Journal of the American Chemical Society* 147:34059–34069

[21] Liu X, Yang Y, Ji W, Liu H, Zhang C, et al. 2007. Controllable growth of nanostructured carbon from coal tar pitch by chemical vapor deposition. *Materials Chemistry and Physics* 104:320–326

[22] Zhang L, Song X, Xiao B, Tan L, Ma H, et al. 2019. Highly graphitized and N, O co-doped porous carbon derived from leaves of viburnum sargenti with outstanding electrochemical performance for effective supercapacitors. *Colloids and Surfaces A: Physicochemical and Engineering Aspects* 580:123721

[23] Li D, Ma J, Xu H, Xu X, Qiu H, et al. 2022. Recycling waste nickel-laden biochar to pseudo-capacitive material by hydrothermal treatment: roles of nickel-carbon interaction. *Carbon Research* 1:16

[24] Nishihara H, Kyotani T. 2018. Zeolite-templated carbons–three-dimensional microporous graphene frameworks. *Chemical Communications* 54:5648–5673

[25] Brun N, Sakaushi K, Yu L, Giebeler L, Eckert J, et al. 2013. Hydrothermal carbon-based nanostructured hollow spheres as electrode materials for high-power lithium–sulfur batteries. *Physical Chemistry Chemical Physics* 15:6080–6087

[26] Li W, Yang Z, Zuo J, Wang J, Li X. 2022. Emerging carbon-based flexible anodes for potassium-ion batteries: progress and opportunities. *Frontiers in Chemistry* 10:1002540

[27] Zhang C, Zhao H, Lei Y. 2020. Recent research progress of anode materials for potassium-ion batteries. *Energy & Environmental Materials* 3:105–120

[28] Lei Y, Li X, Liu L, Ceder G. 2014. Synthesis and stoichiometry of different layered sodium cobalt oxides. *Chemistry of Materials* 26:5288–5296

[29] Liu D, Yang L, Chen Z, Zou G, Hou H, et al. 2020. Ultra-stable Sb confined into N-doped carbon fibers anodes for high-performance potassium-ion batteries. *Science Bulletin* 65:1003−1012

[30] Han X, Gui X, Yi TF, Li Y, Yue C. 2018. Recent progress of $NiCo_2O_4$-based anodes for high-performance lithium-ion batteries. *Current Opinion in Solid State and Materials Science* 22:109−126

[31] Zhang D, Mai YJ, Xiang JY, Xia XH, Qiao YQ, et al. 2012. FeS_2/C composite as an anode for lithium ion batteries with enhanced reversible capacity. *Journal of Power Sources* 217:229−235

[32] Xu Y, Zhang J, Li D. 2020. Recent developments in alloying-type anode materials for potassium-ion batteries. *Chemistry – An Asian Journal* 15:1648−1659

[33] Sultana I, Rahman MM, Chen Y, Glushenkov AM. 2018. Potassium-ion battery anode materials operating through the alloying–dealloying reaction mechanism. *Advanced Functional Materials* 28:1703857

[34] Schon TB, McAllister BT, Li PF, Seferos DS. 2016. The rise of organic electrode materials for energy storage. *Chemical Society Reviews* 45:6345−6404

[35] Zhang Y, Wang Y, Hou L, Yuan C. 2022. Recent progress of carbon-based anode materials for potassium ion batteries. *The Chemical Record* 22:e202200072

[36] Zhang W, Qiu X, Wang C, Zhong L, Fu F, et al. 2022. Lignin derived carbon materials: current status and future trends. *Carbon Research* 1:14

[37] Rajagopalan R, Tang Y, Ji X, Jia C, Wang H. 2020. Advancements and challenges in potassium ion batteries: a comprehensive review. *Advanced Functional Materials* 30:1909486

[38] Liu C, Fang Z, Kou W, Li X, Zhou J, et al. 2026. Synergistic anode design for high-performance potassium ion batteries using hierarchically porous Nb_2C/MoS_2/C composite with an expanded interlayer distance of MoS_2. *Journal of Energy Storage* 144:119841

[39] Silvestre-Albero A, Silvestre-Albero J, Martínez-Escandell M, Rodríguez-Reinoso F. 2014. Micro/mesoporous activated carbons derived from polyaniline: promising candidates for CO_2 adsorption. *Industrial & Engineering Chemistry Research* 53:15398−15405

[40] Wang Q, Gao C, Zhang W, Luo S, Zhou M, et al. 2019. Biomorphic carbon derived from corn husk as a promising anode materials for potassium ion battery. *Electrochimica Acta* 324:134902

[41] Yang J, Ju Z, Jiang Y, Xing Z, Xi B, et al. 2018. Enhanced capacity and rate capability of nitrogen/oxygen dual-doped hard carbon in capacitive potassium-ion storage. *Advanced Materials* 30:1700104

[42] Touja J, Gabaudan V, Farina F, Cavaliere S, Caracciolo L, et al. 2020. Self-supported carbon nanofibers as negative electrodes for K-ion batteries: performance and mechanism. *Electrochimica Acta* 362:137125

[43] Tai Z, Zhang Q, Liu Y, Liu H, Dou S. 2017. Activated carbon from the graphite with increased rate capability for the potassium ion battery. *Carbon* 123:54−61

[44] Zhao W, Deng J, Zhang Q, Luo L, Luo L, et al. 2026. Sustainable balsa-derived polyaniline/activated carbon composites for high-performance asymmetric supercapacitors. *Journal of Energy Storage* 146:120072

[45] Ohzuku T, Iwakoshi Y, Sawai K. 1993. Formation of lithium-graphite intercalation compounds in nonaqueous electrolytes and their application as a negative electrode for a lithium ion (shuttlecock) cell. *Journal of the Electrochemical Society* 140:2490−2498

[46] Thapaliya BP, Luo H, Halstenberg P, Meyer HM, III, Dunlap JR, et al. 2021. Low-cost transformation of biomass-derived carbon to high-performing nano-graphite via low-temperature electrochemical graphitization. *ACS Applied Materials & Interfaces* 13:4393−4401

[47] Tang Z, Wang Y, Zheng Z, Luo X. 2021. *In situ* dual growth of graphitic structures in biomass carbon to yield a potassium-ion battery anode with high initial coulombic efficiency. *Journal of Materials Chemistry A* 9:9191−9202

[48] Hosaka T, Kubota K, Kojima H, Komaba S. 2018. Highly concentrated electrolyte solutions for 4 V class potassium-ion batteries. *Chemical Communications* 54:8387−8390

[49] Xu J, Dou Y, Wei Z, Ma J, Deng Y, et al. 2017. Recent progress in graphite intercalation compounds for rechargeable metal (Li, Na, K, Al)-ion batteries. *Advanced Science* 4:1700146

[50] He G, Mandlmeier B, Schuster J, Nazar LF, Bein T. 2014. Bimodal mesoporous carbon nanofibers with high porosity: freestanding and embedded in membranes for lithium-sulfur batteries. *Chemistry of Materials* 26:3879−3886

[51] Sun S, Yan Q, Wu M, Zhao X. 2021. Carbon aerogel based materials for secondary batteries. *Sustainable Materials and Technologies* 30:e00342

[52] Kobina Sam D, Kobina Sam E, Lv X. 2020. Application of biomass-derived nitrogen-doped carbon aerogels in electrocatalysis and supercapacitors. *ChemElectroChem* 7:3695−3712

[53] Gupta S, Tai NH. 2016. Carbon materials as oil sorbents: a review on the synthesis and performance. *Journal of Materials Chemistry A* 4:1550−1565

[54] Wang J, Xu Z, Eloi JC, Titirici MM, Eichhorn SJ. 2022. Ice-templated, sustainable carbon aerogels with hierarchically tailored channels for sodium-and potassium-ion batteries. *Advanced Functional Materials* 32:2110862

[55] Liu Y, Liu J, Song P. 2021. Recent advances in polysaccharide-based carbon aerogels for environmental remediation and sustainable energy. *Sustainable Materials and Technologies* 27:e00240

[56] Bommier C, Ji X. 2015. Recent development on anodes for Na-ion batteries. *Israel Journal of Chemistry* 55:486−507

[57] El Moctar I, Ni Q, Bai Y, Wu F, Wu C. 2018. Hard carbon anode materials for sodium-ion batteries. *Functional Materials Letters* 11:1830003

[58] Li W, Li Z, Zhang C, Liu W, Han C, et al. 2020. Hard carbon derived from rice husk as anode material for high performance potassium-ion batteries. *Solid State Ionics* 351:115319

[59] Guo Y, Feng Y, Li H, Wang Y, Wen Z, et al. 2022. Carbon quantum dots in hard carbon: an approach to achieving PIB anodes with high potassium adsorption. *Carbon* 189:142−151

[60] Zhao LF, Hu Z, Lai WH, Tao Y, Peng J, et al. 2021. Hard carbon anodes: fundamental understanding and commercial perspectives for Na-ion batteries beyond Li-ion and K-ion counterparts. *Advanced Energy Materials* 11:2002704

[61] Yu Q, Shi X, Zhang T, Zhao Y, Jin J, et al. 2026. Hollow carbon fibers with balanced graphitization and defects for extremely fast-charging potassium storage. *Nano Research* 19:94908253

[62] Bai M, Xie K, Yuan K, Zhang K, Li N, et al. 2018. A scalable approach to dendrite-free lithium anodes via spontaneous reduction of spray-coated graphene oxide layers. *Advanced Materials* 30:1801213

[63] Xiong P, Zhao X, Xu Y. 2018. Nitrogen-doped carbon nanotubes derived from metal–organic frameworks for potassium-ion battery anodes. *ChemSusChem* 11:202−208

[64] Jiang Y, Hu M, Zhang D, Yuan T, Sun W, et al. 2014. Transition metal oxides for high performance sodium ion battery anodes. *Nano Energy* 5:60−66

[65] Khan N, Han G, Ali Mazari S. 2022. Carbon nanotubes-based anode materials for potassium ion batteries: a review. *Journal of Electroanalytical Chemistry* 907:116051

[66] Li S, Qin J, Gao T, Du J, Yuan K, et al. 2022. Fabrication of Fe_3C nanoparticles embedded in N-doped carbon nanotubes/porous carbon 3D materials derived from distilled grains for high performance of potassium ion battery. *Journal of Alloys and Compounds* 912:165130

[67] Zhang R, Zhang Y, Wei F. 2017. Horizontally aligned carbon nanotube arrays: growth mechanism, controlled synthesis, characterization, properties and applications. *Chemical Society Reviews* 46:3661−3715

[68] Mathangi JB, Kalavathy MH. 2022. A comparative study of carbon nanotube characteristics synthesized from various biomass precursors through hydrothermal techniques and their potential applications. *Chemical Engineering Communications* 209:127−139

[69] Xiang Y, Xu L, Yang L, Ye Y, Ge Z, et al. 2022. Natural stibnite for lithium-/sodium-ion batteries: carbon dots evoked high initial coulombic efficiency. *Nano-Micro Letters* 14:136

[70] Wang D, Wang Q, Tan M, Wang S, Luo S, et al. 2022. Biomass CQDs derivate carbon as high-performance anode for K-ion battery. *Journal of Alloys and Compounds* 922:166260

[71] Jin L, Shen C, Wu Q, Shellikeri A, Zheng J, et al. 2021. Pre-lithiation strategies for next-generation practical lithium-ion batteries. *Advanced Science* 8:2005031

[72] Chen S, Qiu L, Cheng HM. 2020. Carbon-based fibers for advanced electrochemical energy storage devices. *Chemical Reviews* 120:2811−2878
[73] Fang W, Yang S, Yuan TQ, Charlton A, Sun RC. 2017. Effects of various surfactants on alkali lignin electrospinning ability and spun fibers. *Industrial & Engineering Chemistry Research* 56:9551−9559
[74] Cheng D, Li Y, Zhang J, Tian M, Wang B, et al. 2020. Recent advances in electrospun carbon fiber electrode for vanadium redox flow battery: properties, structures, and perspectives. *Carbon* 170:527−542
[75] Zhang W, Miao W, Liu X, Li L, Yu Z, et al. 2018. High-rate and ultralong-stable potassium-ion batteries based on antimony-nanoparticles encapsulated in nitrogen and phosphorus co-doped mesoporous carbon nanofibers as an anode material. *Journal of Alloys and Compounds* 769:141−148
[76] Jiang H, Huang L, Wei Y, Wang B, Wu H, et al. 2019. Bio-derived hierarchical multicore–shell Fe_2N-nanoparticle-impregnated n-doped carbon nanofiber bundles: a host material for lithium-/potassium-ion storage. *Nano-Micro Letters* 11:56
[77] Zhang Y, Huang Z, Zhang H, Zhang Q, Zhang J, et al. 2021. Nitrogen-doped porous biomass carbon with ultrastable performance as anodes for potassium-ion batteries. *Nano Select* 2:810−816
[78] Wu Y, Gao X, Nguyen TT, Wu J, Guo M, et al. 2022. Green and low-cost natural lignocellulosic biomass-based carbon fibers-processing, properties, and applications in sports equipment: a review. *Polymers* 14:2591
[79] Ye R, Chyan Y, Zhang J, Li Y, Han X, et al. 2017. Laser-induced graphene formation on wood. *Advanced Materials* 29:201702211
[80] Shah J, Lopez-Mercado J, Carreon MG, Lopez-Miranda A, Carreon ML. 2018. Plasma synthesis of graphene from mango peel. *ACS Omega* 3:455−463
[81] Cao X, Ma L, Gao B, Harris W. 2009. Dairy-manure derived biochar effectively sorbs lead and atrazine. *Environmental Science & Technology* 43:3285−3291
[82] Mohan D, Pittman CU, Steele PH. 2006. Pyrolysis of wood/biomass for bio-oil: a critical review. *Energy & Fuels* 20:848−889
[83] Rawat S, Mishra RK, Bhaskar T. 2022. Biomass derived functional carbon materials for supercapacitor applications. *Chemosphere* 286:131961
[84] Bergius F. 1913. Production of hydrogen from water and coal from cellulose at high temperatures and pressures. *Journal of the Society of Chemical Industry* 32:462−467
[85] Funke A, Ziegler F. 2010. Hydrothermal carbonization of biomass: a summary and discussion of chemical mechanisms for process engineering. *Biofuels, Bioproducts and Biorefining* 4:160−177
[86] Khan TA, Saud AS, Jamari SS, Rahim MHA, Park JW, et al. 2019. Hydrothermal carbonization of lignocellulosic biomass for carbon rich material preparation: a review. *Biomass and Bioenergy* 130:105384
[87] Liu Z, Zhang FS, Wu J. 2010. Characterization and application of chars produced from pinewood pyrolysis and hydrothermal treatment. *Fuel* 89:510−514
[88] Qiu T, Cao W, Xie K, Ahmad F, Zhao W, et al. 2025. CO_2 capture performances of H_3PO_4/KOH activated microwave pyrolyzed porous biochar. *Sustainable Carbon Materials* 1:e004
[89] Zhu L, Lei H, Wang L, Yadavalli G, Zhang X, et al. 2015. Biochar of corn stover: microwave-assisted pyrolysis condition induced changes in surface functional groups and characteristics. *Journal of Analytical and Applied Pyrolysis* 115:149−156
[90] Hoseinzadeh Hesas R, Wan Daud WMA, Sahu JN, Arami-Niya A. 2013. The effects of a microwave heating method on the production of activated carbon from agricultural waste: a review. *Journal of Analytical and Applied Pyrolysis* 100:1−11
[91] Qiu T, Xie K, Liu C, Ahmad F, Zhao W, et al. 2025. Microwave-assisted pyrolysis for advanced sustainable carbon materials. *Sustainable Carbon Materials* 1:e011
[92] Bartoli M, Rosi L, Giovannelli A, Frediani P, Frediani M. 2020. Characterization of bio-oil and bio-char produced by low-temperature microwave-assisted pyrolysis of olive pruning residue using various absorbers. *Waste Management & Research* 38:213−225
[93] Luque R, Menéndez JA, Arenillas A, Cot J. 2012. Microwave-assisted pyrolysis of biomass feedstocks: the way forward? *Energy & Environmental Science* 5:5481−5488
[94] Nabais JV, Carrott P, Ribeiro Carrott MML, Luz V, Ortiz AL. 2008. Influence of preparation conditions in the textural and chemical properties of activated carbons from a novel biomass precursor: the coffee endocarp. *Bioresource Technology* 99:7224−7231
[95] Sevilla M, Díez N, Fuertes AB. 2021. More sustainable chemical activation strategies for the production of porous carbons. *ChemSusChem* 14:94−117
[96] Zhang H, Zhang Y, Bai L, Zhang Y, Sun L. 2021. Effect of physiochemical properties in biomass-derived materials caused by different synthesis methods and their electrochemical properties in supercapacitors. *Journal of Materials Chemistry A* 9:12521−12552
[97] Dos Reis GS, Larsson SH, de Oliveira HP, Thyrel M, Lima EC. 2020. Sustainable biomass activated carbons as electrodes for battery and supercapacitors—a mini-review. *Nanomaterials* 10:1398

Copyright: © 2026 by the author(s). Published by Maximum Academic Press, Fayetteville, GA. This article is an open access article distributed under Creative Commons Attribution License (CC BY 4.0), visit https://creativecommons.org/licenses/by/4.0/.